Electronic Supplementary Material (ESI) for Chemical Communications.

Supporting Information

for

A Hyaluronidase/Temperature Dual-Responsive Supramolecular Assembly Based on the Anionic Recognition of Calixpyridinium

Kui Wang,* Jian-Hua Cui, Si-Yang Xing,* and Xiao-Wei Ren

Tianjin Key Laboratory of Structure and Performance for Functional Molecules, Key Laboratory of Inorganic-Organic Hybrid Functional Materials Chemistry (Tianjin Normal University), Ministry of Education, College of Chemistry, Tianjin Normal University, Tianjin 300387, China

Experimental Section

Materials

Hyaluronan (HA, MW = 77 kDa) was purchased from Shandong Freda Biopharm Co., Ltd, and the concentration of HA could be calculated based on this value. 1-Methylpyridinium chloride was purchased from TCI. Hyaluronidase (HAase) from bovine tests (Type I-S, lyophilized powder, 400–1000 units/mg solid) and Nile red were purchased from Sigma–Aldrich. All of these compounds were used without further purification. Calixpyridinium was synthesized and purified according to a previously reported procedure.[1] An aqueous solution of 3-bromomethylpyridinium bromide (2.0 g, 8 mmol) was neutralized with $NaHCO_3$ and the resulting 3-bromomethylpyridine was immediately extracted in CH_2Cl_2 (60 mL×3). When the solvent was evaporated at room temperature, N-alkylation vigorously occurred to yield a mixture of quaternary pyridinium salts. Calixpyridinium was isolated by recrystallization from water (99 mg, 0.14 mmol). It was identified by ^1H (Fig. S25) and ^{13}C (Fig. S26) NMR spectroscopy in D_2O, performed on a Bruker AV400 spectrometer, and by X-ray crystallographic analysis (Fig. S27), performed on a Bruker APEX-II CCD diffractometer. Preparation of the calixpyridinium–HA supramolecular assembly: HA was first dissolved in double-distilled water, and then calixpyridinium solution was dropwise mingled with the HA solution to get the dynamic calixpyridinium–HA supramolecular assembly. The resulting concentrations of calixpyridinium and HA are 0.10 mM and 1.40 μM, respectively. The formation of the calixpyridinium–HA supramolecular assembly would achieve balance in about 1 h.

The aqueous solution was adjusted to different pH values by HCl or NaOH. The pH values were verified on a Sartorius pp-20 pH meter calibrated with two standard buffer solutions.

UV/Vis spectra

UV/Vis spectra and the optical transmittance of the aqueous solution were measured in a quartz cell (light path 10 mm) on a Shimadzu UV-2600 spectrophotometer.

High-resolution TEM experiments

High-resolution TEM images were acquired using a Tecnai G^2 F20 high-resolution transmission electron microscope operating at an accelerating voltage of 200 keV.

SEM experiments

SEM images were recorded on a FEI Nova Nano 230 scanning electron microscope.

DLS measurements

DLS experiments were measured by NanoBrook 173 Plus at scattering angle of 90°.

Results and Discussion

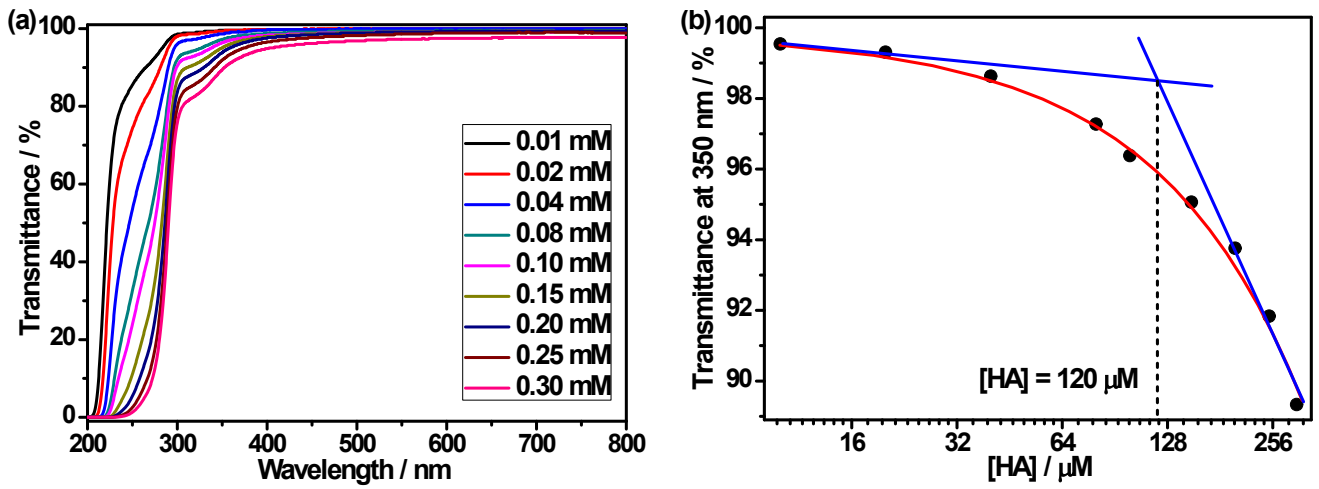

Fig. S1 (a) Optical transmittance of aqueous solutions of HA at different concentrations from 0.01 to 0.30 mM at room temperature. (b) Dependence of the optical transmittance at 350 nm on HA concentration.

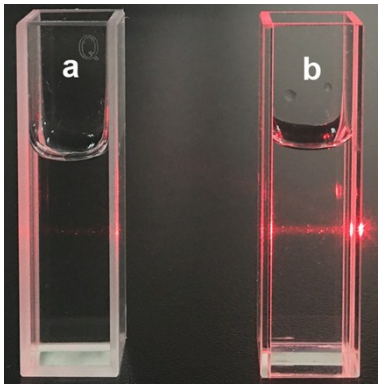

Fig. S2 Photos showing the Tyndall effect of free HA at different concentrations, [HA] = 78 μM (a) and [HA] = 156 μM (b).

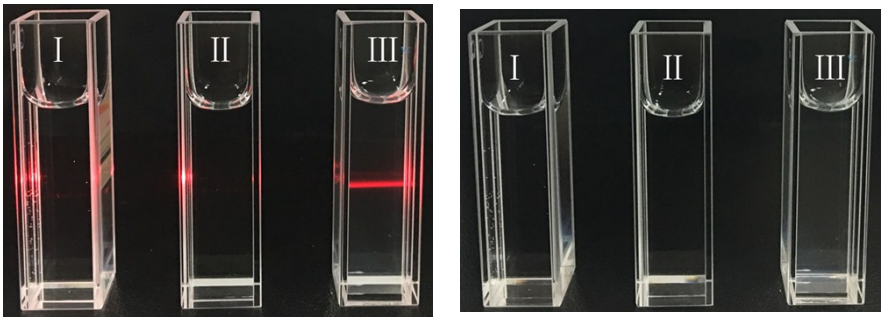

Fig. S3 Photos showing the Tyndall effect (a) and turbidity (b) of free calixpyridinium (I), free HA (II), and calixpyridinium–HA complex (III) in water, [calixpyridinium] = 0.10 mM, and [HA] = 1.40 μM.

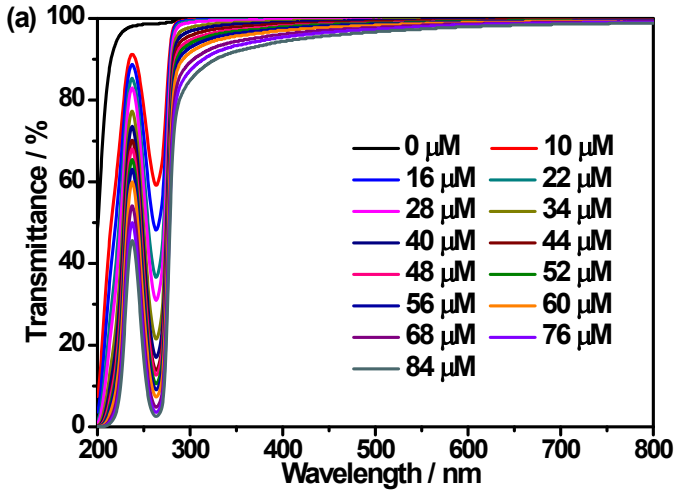

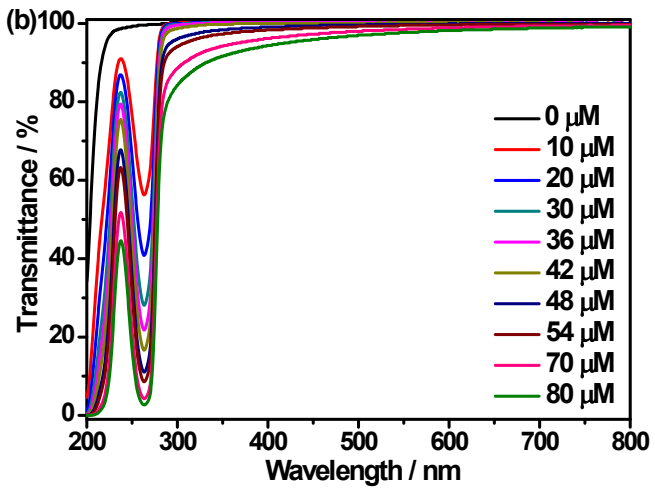

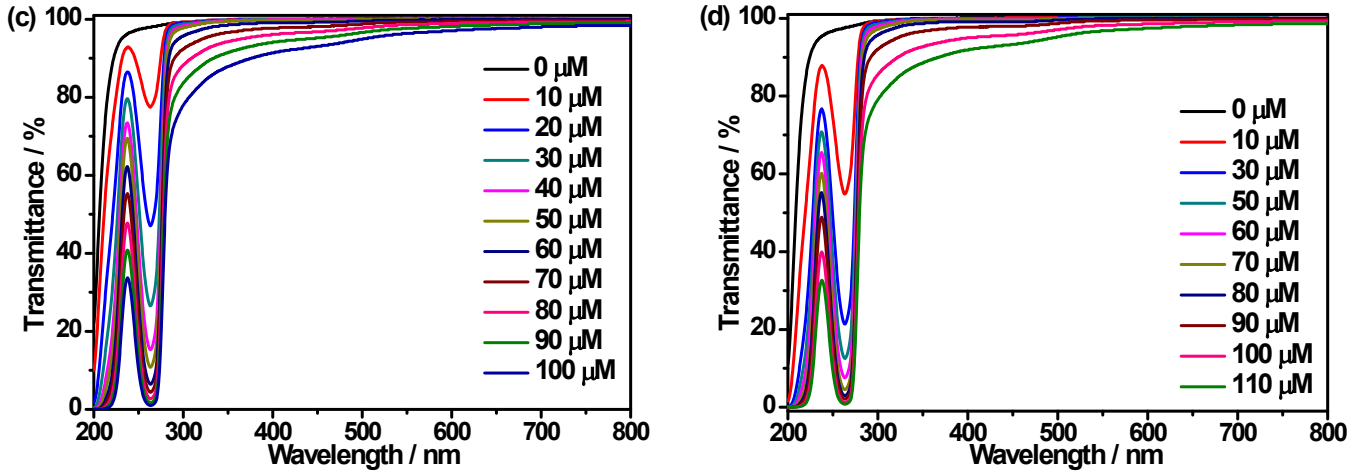

Fig. S4 Optical transmittance of aqueous solutions of calixpyridinium at different concentrations in the presence of 0.52 μM (a), 0.78 μM (b), 0.99 μM (c), and 1.56 μM (d) HA.

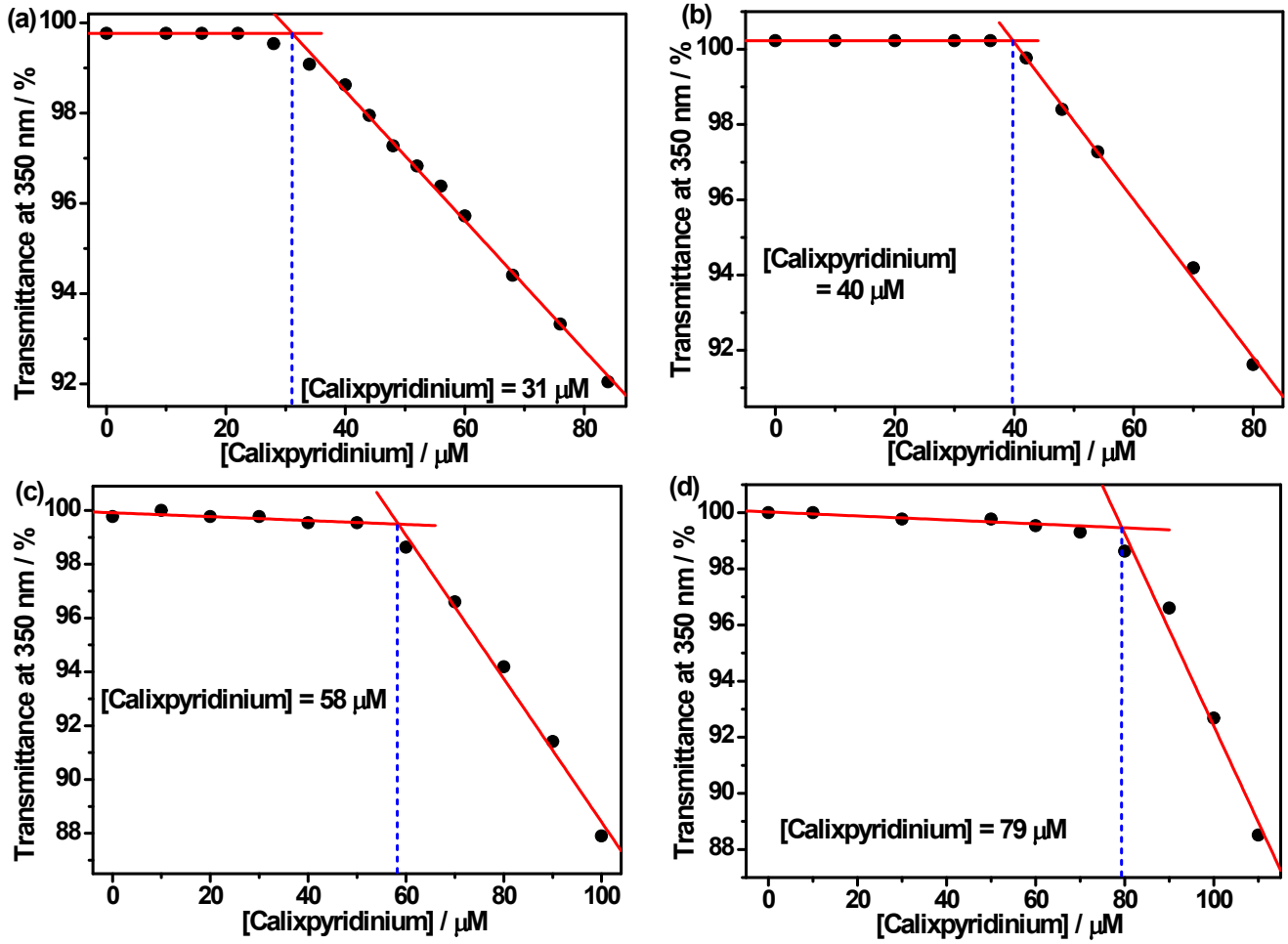

Fig. S5 Dependence of the optical transmittance at 350 nm on calixpyridinium concentration in the presence of 0.52 μM (a), 0.78 μM (b), 0.99 μM (c), and 1.56 μM (d) HA.

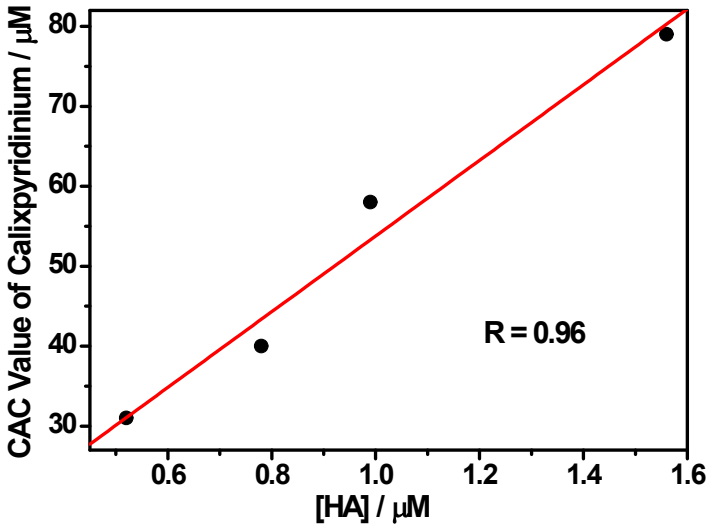

Fig. S6 Linear relationship between the CAC values of calixpyridinium and the concentrations of HA in water.

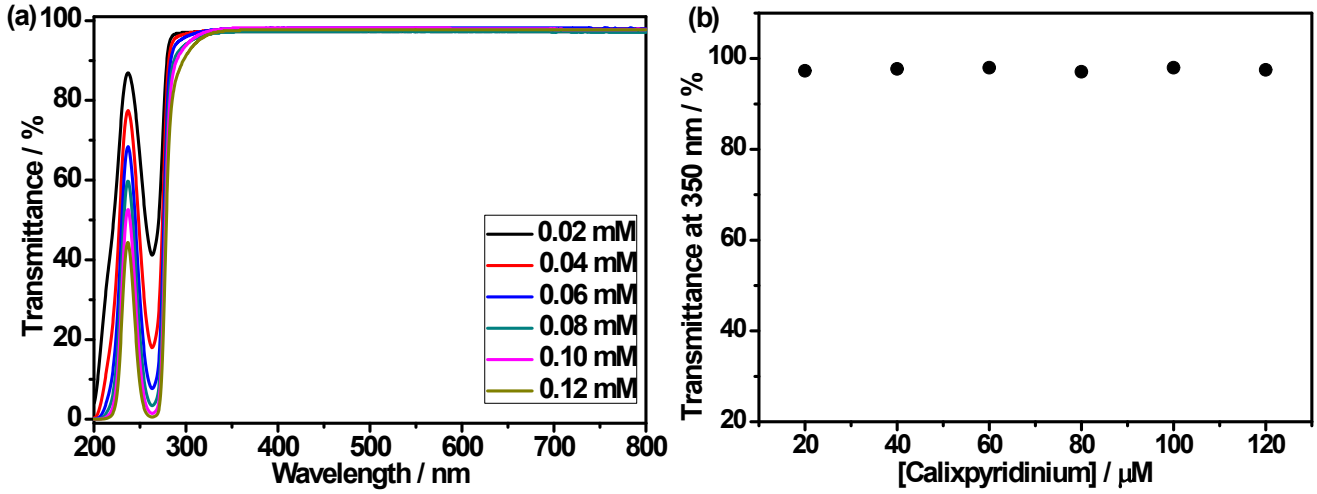

Fig. S7 (a) Optical transmittance of aqueous solutions of calixpyridinium at different concentrations from 20 to 120 μM at room temperature. (b) Dependence of the optical transmittance at 350 nm on calixpyridinium concentration.

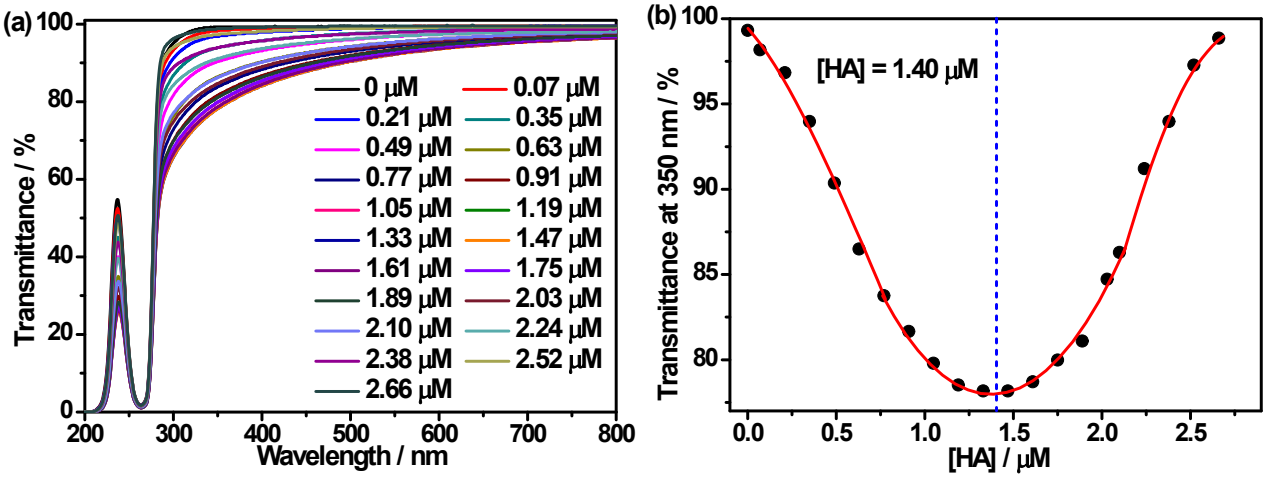

Fig. S8 (a) Optical transmittance of calixpyridinium (0.10 mM) by increasing the concentration of HA from 0 to 2.66 μM at room temperature in water. (b) Dependence of the optical transmittance at 350 nm on the HA concentration with a fixed calixpyridinium concentration of 0.10 mM.

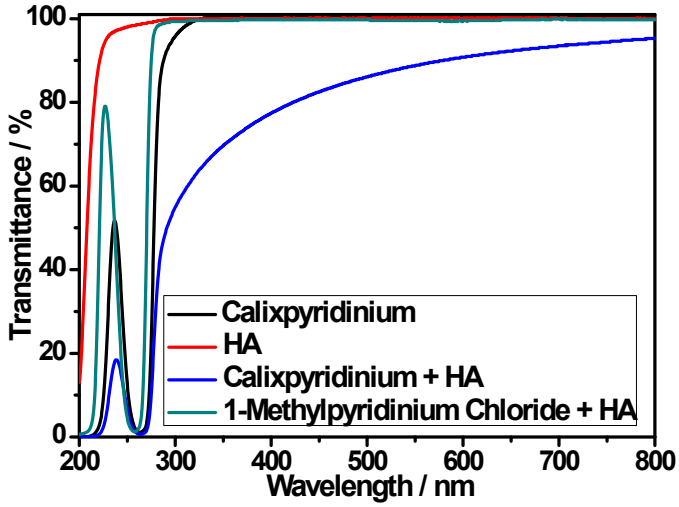

Fig. S9 Optical transmittance of calixpyridinium, HA, calixpyridinium+HA, and 1-methylpyridinium+HA at room temperature in water, [calixpyridinium] = 0.10 mM, [HA] = 1.40 μM, and [1-methylpyridinium chloride] = 0.45 mM.

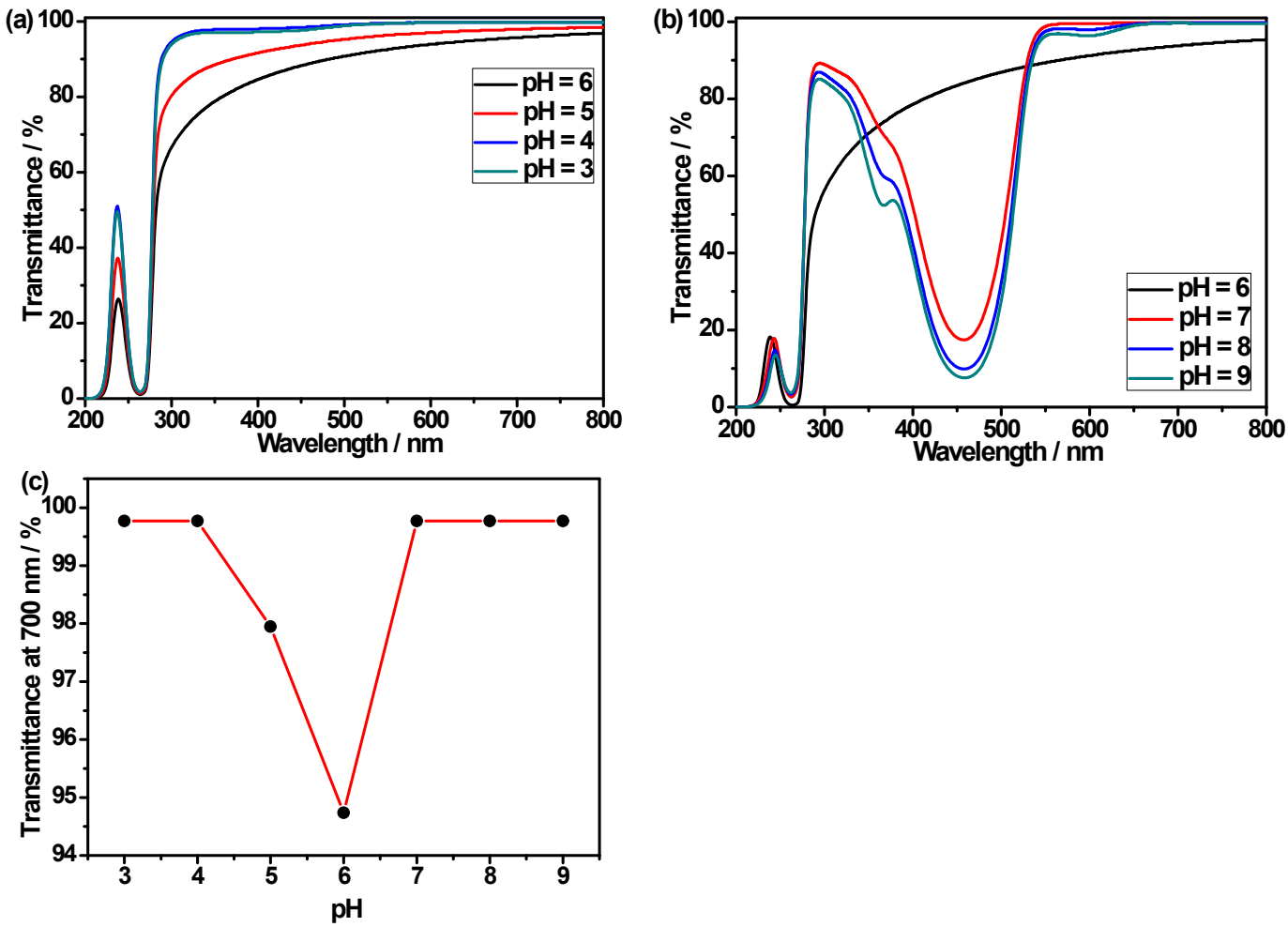

Fig. S10 (a and b) Optical transmittance of the aqueous solutions of the calixpyridinium-HA assembly at different pH values, [calixpyridinium] = 0.10 mM, and [HA] = 1.40 μM. (c) Dependence of the optical transmittance at 700 nm on the pH values of the calixpyridinium-HA aqueous solutions.

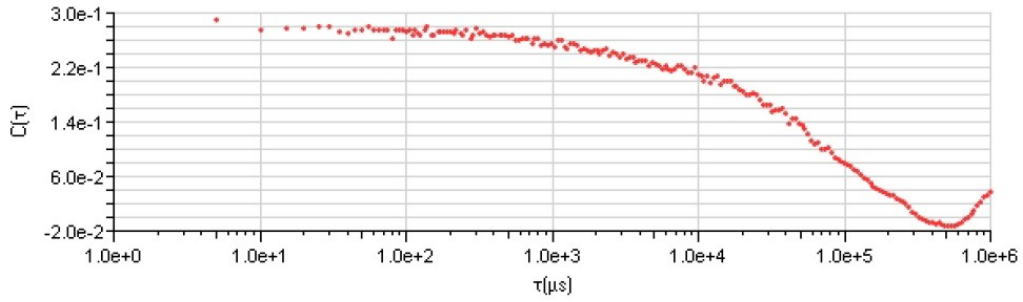

(a)

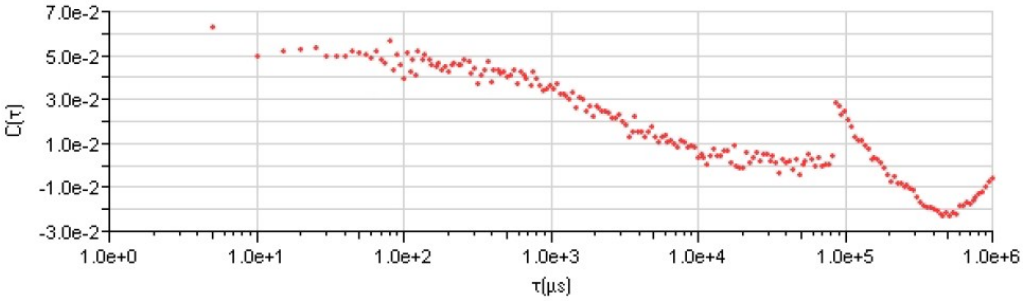

(b)

Fig. S11 DLS data of calixpyridinium (a) and HA (b), [calixpyridinium] = 0.10 mM, and [HA] = 1.40 μM.

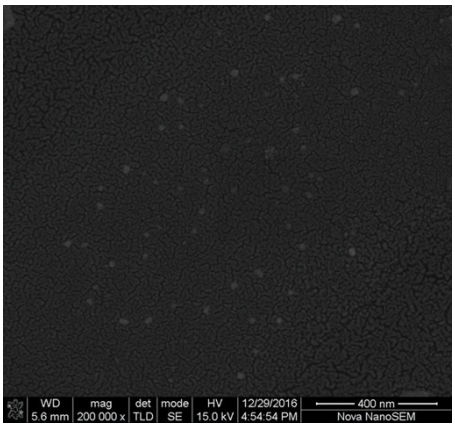

(a)

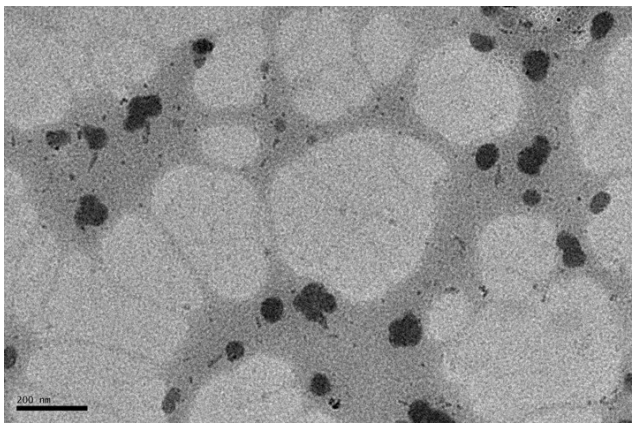

(b)

Fig. S12 SEM (a) and high-resolutionTEM (b) images of the calixpyridinium–HA assembly, [calixpyridinium] = 0.10 mM, and [HA] = 1.40 μM.

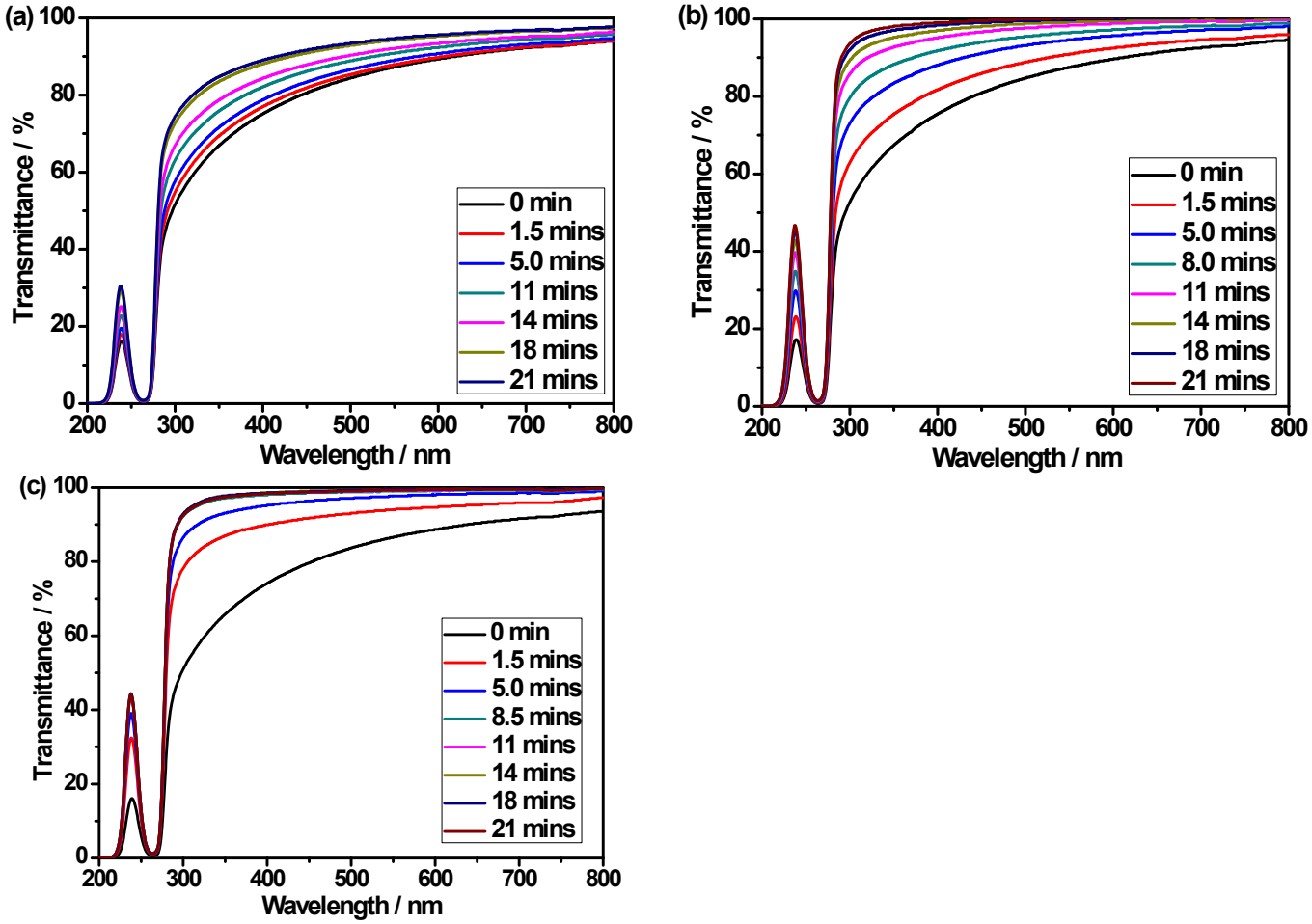

Fig. S13 Optical transmittance of the calixpyridinium–HA assembly at different time after addition of 1 U/mL (a), 3 U/mL (b), and 10 U/mL (c) HAase in water at 37 °C, [calixpyridinium] = 0.10 mM, and [HA] = 1.40 μM.

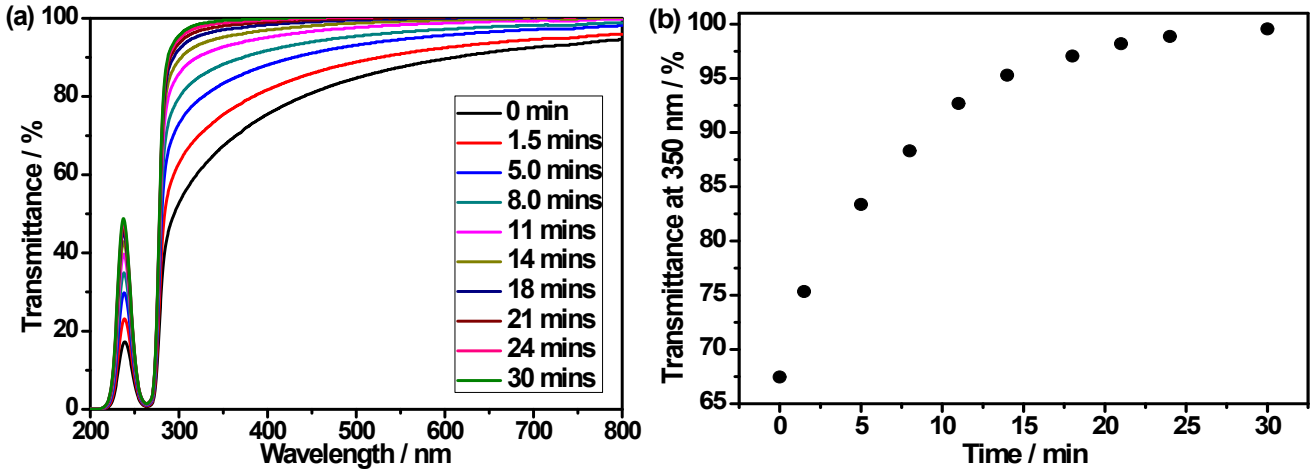

Fig. S14 (a) Optical transmittance of the calixpyridinium–HA assembly at different time after addition of 3 U/mL HAase in water at 37 °C. (b) Dependence of the optical transmittance of the calixpyridinium–HA solution at 350 nm on time in the presence of 3 U/mL HAase. [calixpyridinium] = 0.10 mM, and [HA] = 1.40 μM.

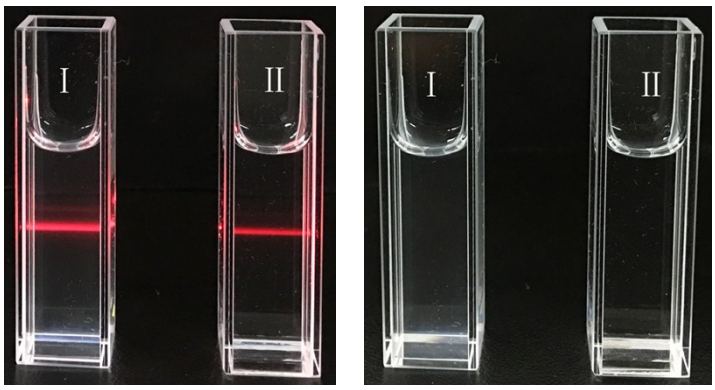

(a) (b)

Fig. S15 Photos showing the Tyndall effect (a) and turbidity (b) of the calixpyridinium–HA assembly before (I) and after addition of HAase for 30 minutes (II), [calixpyridinium] = 0.10 mM, [HA] = 1.40 μM, and [HAase] = 10 U/mL.

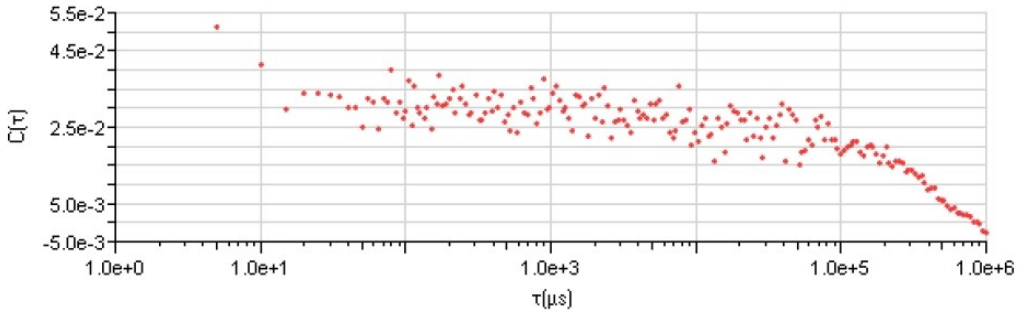

Fig. S16 DLS data of the calixpyridinium–HA assembly after addition of HAase for 30 minutes, [calixpyridinium] = 0.10 mM, [HA] = 1.40 μM, and [HAase] = 10 U/mL.

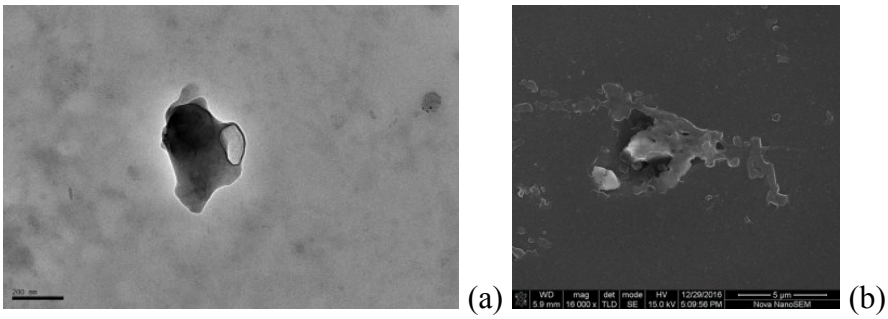

(a) (b)

Fig. S17 High-resolution TEM (a) and SEM (b) images of the calixpyridinium–HA assembly after addition of 10 U/mL HAase for 30 minutes.

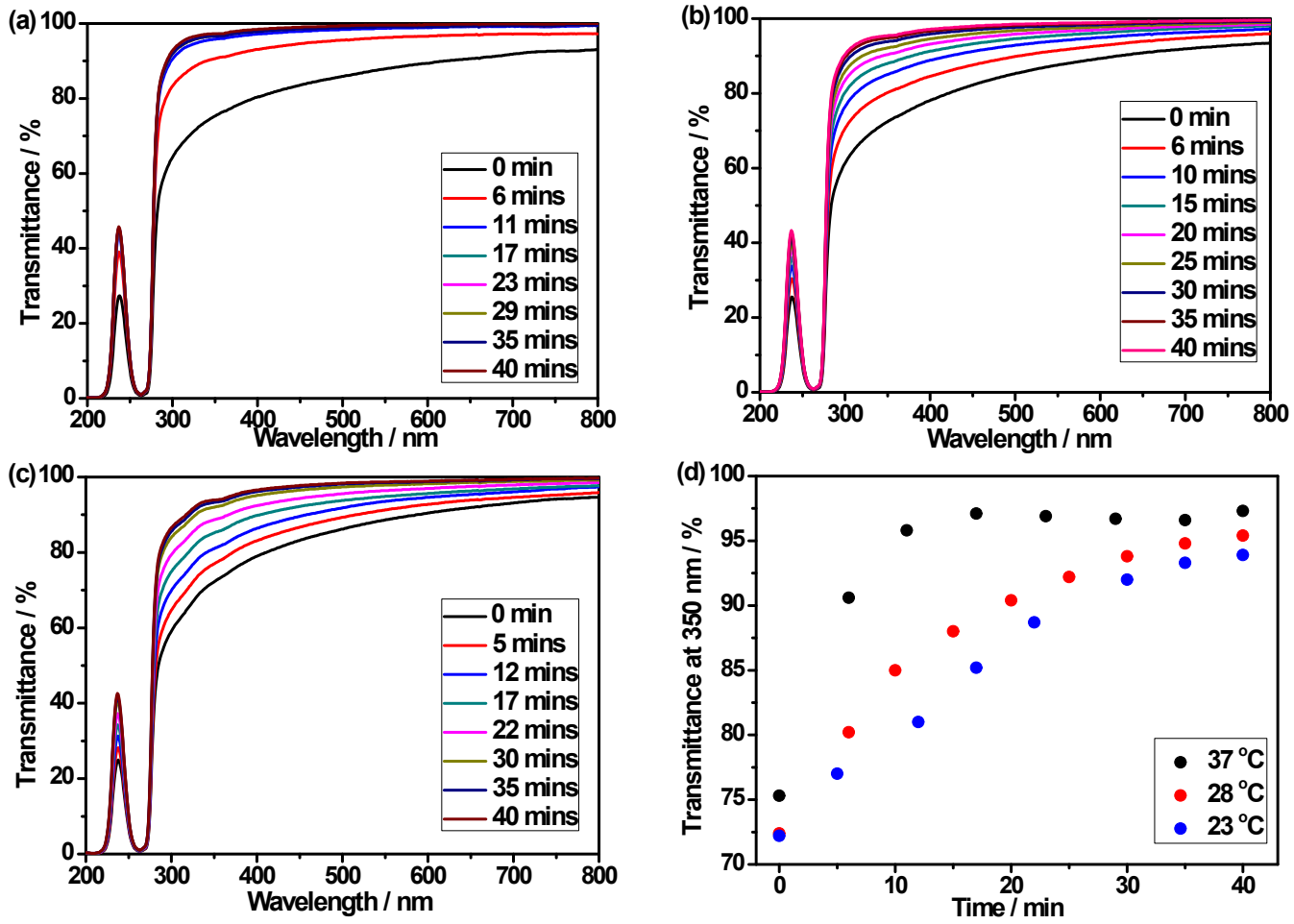

Fig. S18 Optical transmittance of the calixpyridinium–HA assembly at different time after addition of 10 U/mL HAase in water at 37 °C (a), 28 °C (b) and 23 °C (c). (d) Dependence of the optical transmittance of the calixpyridinium–HA solution at 350 nm on time in the presence of 10 U/mL HAase at different temperatures in water. [calixpyridinium] = 0.10 mM, and [HA] = 1.40 μM.

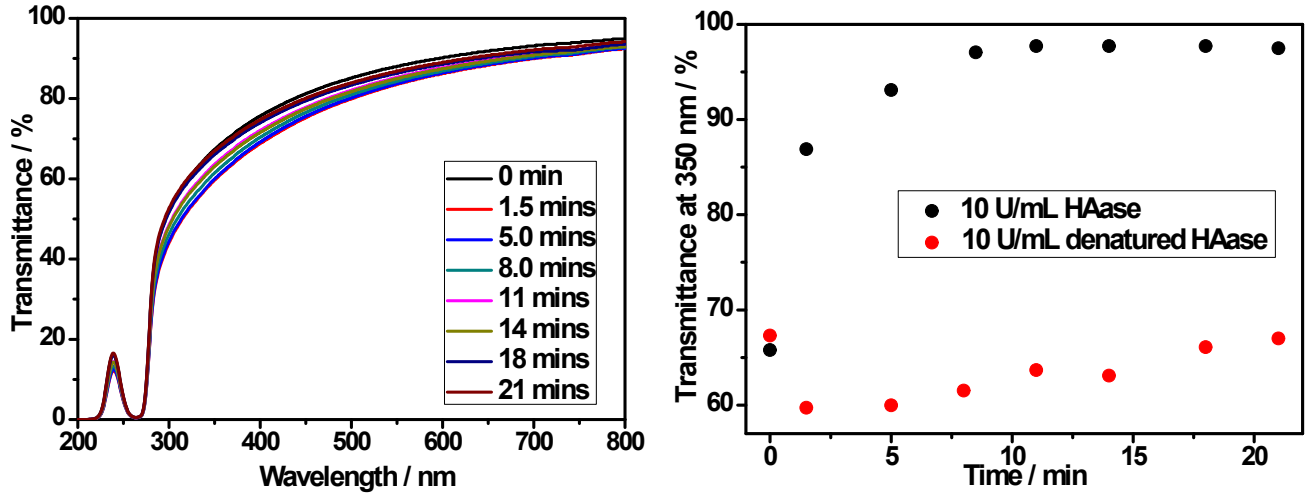

(a) (b)

(c) (d)

Fig. S19 (a) Optical transmittance of the calixpyridinium–HA assembly at different time after addition of 10 U/mL denatured HAase in water at 37 °C. (b) Dependence of the optical transmittance of the calixpyridinium–HA assembly at 350 nm on time in the presence of 10 U/mL HAase and denatured HAase. Photos showing the Tyndall effect (c) and turbidity (d) of the calixpyridinium–HA assembly before (I) and after addition of denatured HAase for 30 minutes (II). [calixpyridinium] = 0.10 mM, and [HA] = 1.40 μM.

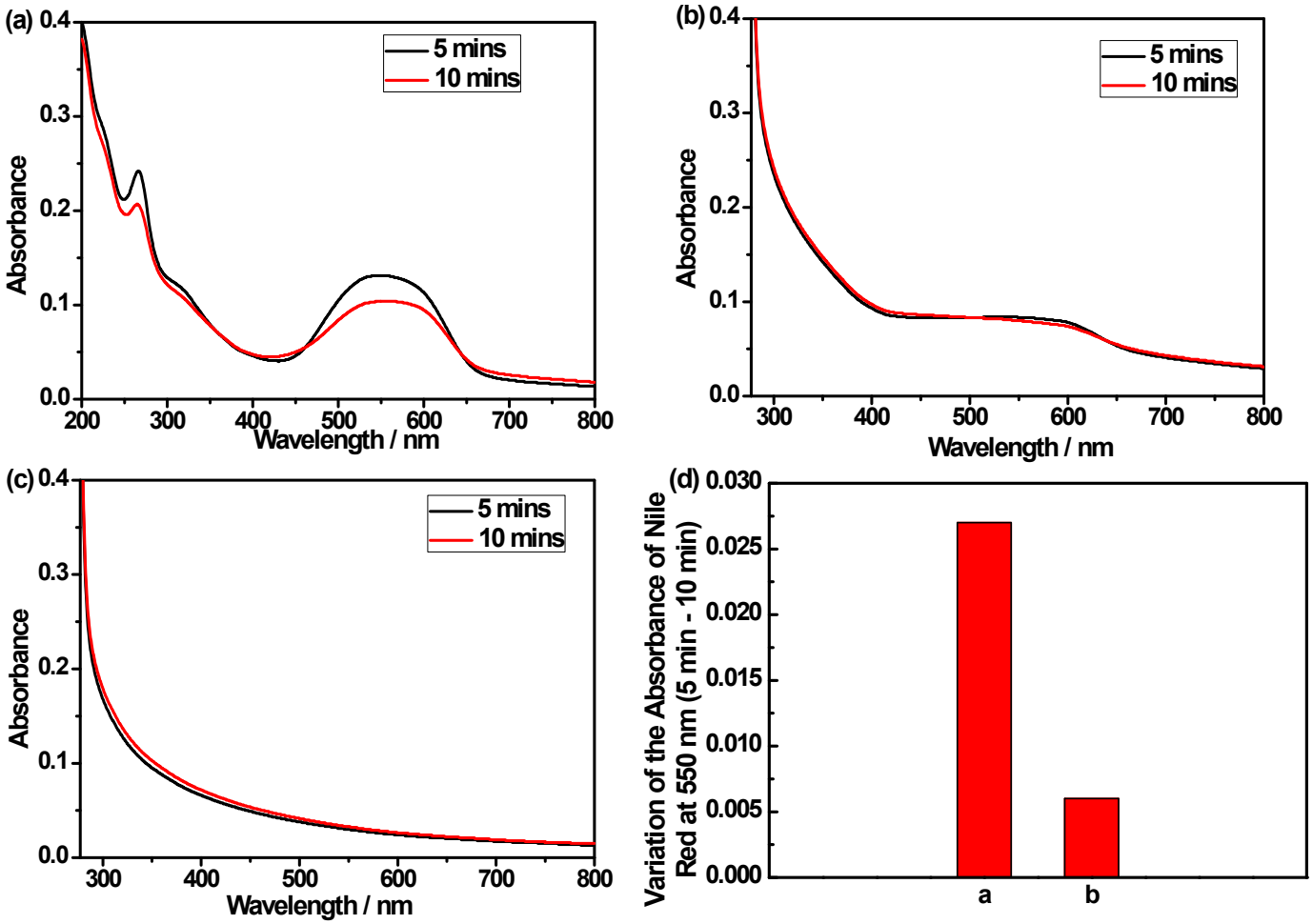

Fig. S20 UV-vis absorption spectra of aqueous solutions of Nile red in the absence (a) and presence (b) of the calixpyridinium–HA assembly at 5 and 10 minutes after preparation. (c) UV-vis absorption spectra of the aqueous solutions of the calixpyridinium–HA assembly at 5 and 10 minutes after preparation. (d) The variation of the absorbance of Nile red at 550 nm (5 mins – 10 mins; a: Nile red in aqueous solution; b: Nile red in the aqueous solution of the calixpyridinium–HA assembly). [calixpyridinium] = 0.10 mM, [HA] = 1.40 μM, and [Nile red] = 4.39 μM; the mother liquor of Nile red was prepared at 1.10 mM in absolute ethyl alcohol.

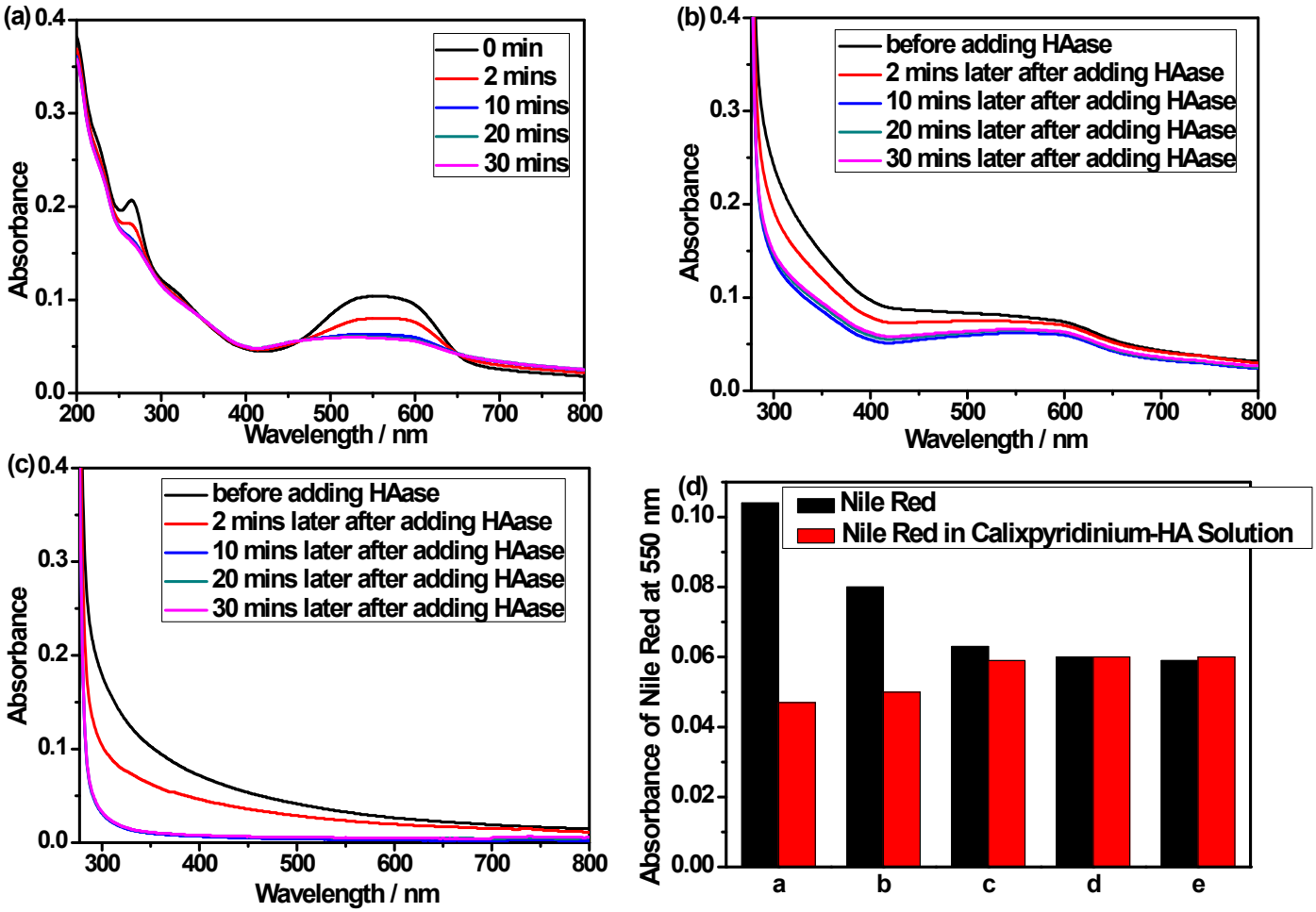

Fig. S21 (a) UV-vis absorption spectra of the aqueous solutions of Nile red at different time after preparation. UV-vis absorption spectra of the aqueous solutions of the calixpyridinium–HA assembly in the presence (b) and absence (c) of Nile red before and at different time after adding HAase. (d) The absorbance of Nile red in aqueous solution at 550 nm at different time after preparation, and the absorbance of Nile red in the calixpyridinium–HA solution at 550 nm before and at different time after adding HAase (a: 0 minute and before adding HAase; b: 2 minutes and 2 minutes later after adding HAase; c: 10 minutes and 10 minutes later after adding HAase; d: 20 minutes and 20 minutes later after adding HAase; e: 30 minutes and 30 minutes later after adding HAase). [calixpyridinium] = 0.10 mM, [HA] = 1.40 μM, [HAase] = 10 U/mL, and [Nile red] = 4.39 μM; the mother liquor of Nile red was prepared at 1.10 mM in absolute ethyl alcohol.

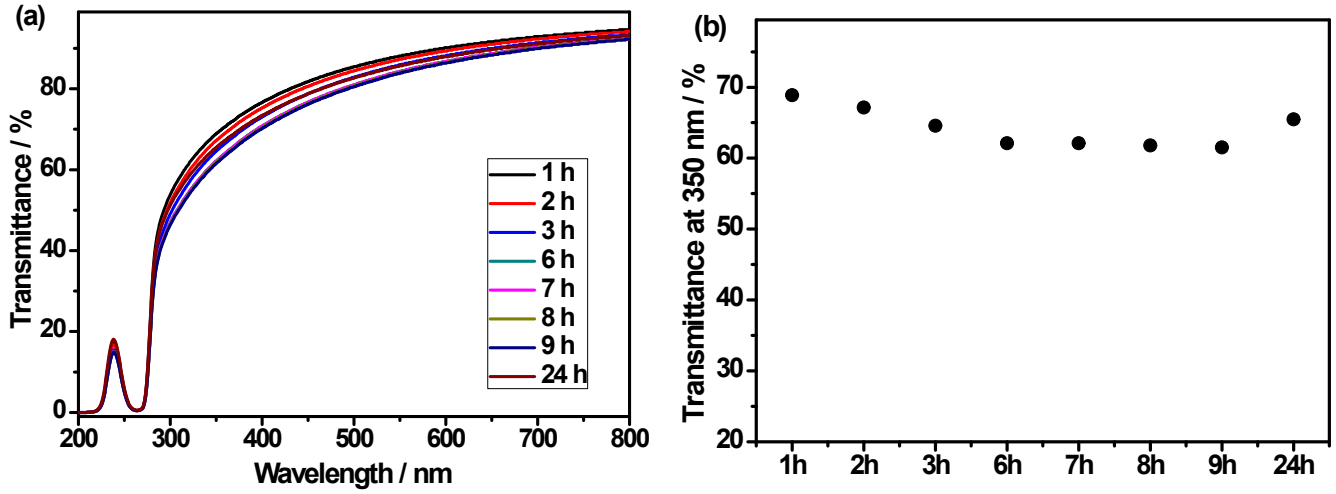

Fig. S22 (a) Optical transmittance of the calixpyridinium–HA assembly at different time within 24 h at room temperature in water. (b) Dependence of the optical transmittance at 350 nm on time. [calixpyridinium] = 0.10 mM, and [HA] = 1.40 μM.

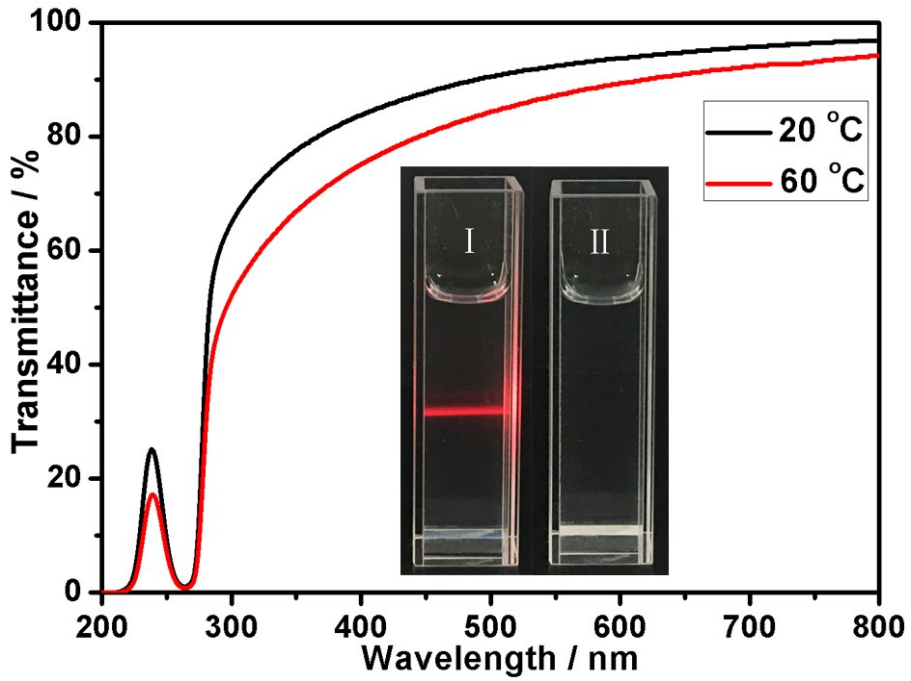

Fig. S23 Optical transmittance of the calixpyridinium–HA assembly at 20 and 60 °C in water. Inset: photos showing the Tyndall effect (I) and turbidity (II) of the calixpyridinium-HA assembly at 60 °C in water. [calixpyridinium] = 0.10 mM, and [HA] = 1.40 μM.

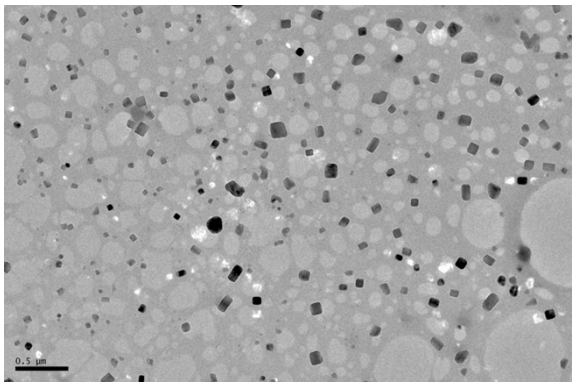

Fig. S24 High-resolution TEM image of the calixpyridinium–HA assembly prepared at 60 °C, [calixpyridinium] = 0.10 mM, and [HA] = 1.40 μM.

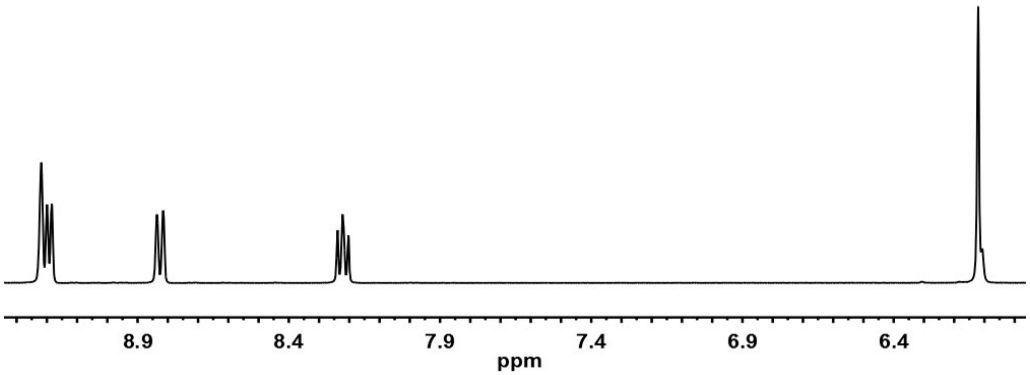

Fig. S25 ^{1}H NMR spectrum of calixpyridinium in D_2O.

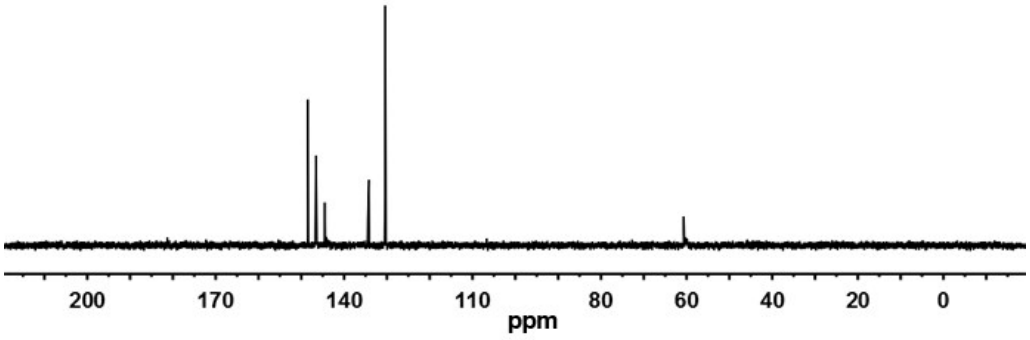

Fig, S26 ^{13}C NMR spectrum of calixpyridinium in D_2O.

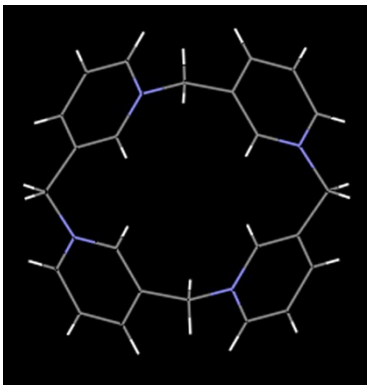

Fig. S27 Crystal structure of calixpyridinium. It is in accordance with the previous reported crystal structure of calixpyridinium.[1]

References

1 S. Shinoda, M. Tadokoro, H. Tsukube and R. Arakawa, *Chem. Commun.*, 1998, 181−182.